Surface & Coatings Technology 206 (2011) 1449–1453

Contents lists available at SciVerse ScienceDirect

Surface & Coatings Technology

journal homepage: www.elsevier.com/locate/surfcoat

Influence of gas flow on argon microwave plasma jet at atmospheric pressure

Shouichiro Iio [a,*], Kosuke Yanagisawa [a], Chizuru Uchiyama [a], Katsuya Teshima [a], Naomichi Ezumi [b], Toshihiko Ikeda [a]

[a] Department of Environmental Science and Technology, Shinshu University, Wakasato 4-17-1, Nagano-shi, Nagano 380-8553, Japan
[b] Nagano National College of Technology, Tokuma 716, Nagano-shi, Nagano 381-8550, Japan

ARTICLE INFO

Article history:
Received 22 December 2010
Accepted in revised form 9 September 2011
Available online 17 September 2011

Keywords:
Plasma jet
Atmospheric pressure
Microwave discharge
Argon
Flow visualization
Velocity measurement

ABSTRACT

Many kinds of an atmospheric-pressure plasma jet have been developed and used for widespread applications such as a surface treatment and modified. This study focused on the argon atmospheric-pressure microplasma jet generated by discharging of RF power of 2.45 GHz microwave. The plasma jet shows sensitivity to surrounding environment: pressure, temperature and gaseous species. It is therefore absolutely imperative that a nature of atmospheric-pressure plasma jet should be understood from a point of fluid dynamics. This study, therefore, focused on the interrelationship between the plasma jet and the working gas. Motion of the plasma jet and the working gas was evaluated by velocity measurement and fast photography. As a result, the unsteady sinusoidal waving motion in the radial direction of a torch was observed. Advection velocity of the plasma in just downstream region of the torch exit increases with the supplying flow rate, and the velocity ratio is in the range of 0.75–0.87.

1. Introduction

Atmospheric-pressure plasmas are used in many fields such as electrical engineering, chemical engineering, and materials engineering. The properties of atmospheric-pressure plasmas are discussed in many books and publications [1–4]. This high-pressure plasma including the atmospheric-pressure plasma has advantage with respect to cost and consumption energy since it can be produced without using any vacuum equipment, which is essential for producing low-pressure plasma. Further, the unique reactions occurring in atmospheric-pressure plasma are attracting considerable attention. Atmospheric-pressure plasma has been studied extensively [5] and is used in the areas of biotechnology, medical treatment [6–10], remediation of pollutants [7,11], nanotechnology [12,13], and surface processing [14,15]. C. Oliveira et al. [14] investigated an argon–hydrogen atmospheric pressure microplasma jet for the treatment of materials; they clarified that Ar–H_2 microplasma jet powered by a commercial RF power source was employed to generate long non-thermal microplasma reaching up to 30 mm, which may be a suitable source of active chemical species. Surprising hot hydrogen atoms were found along the atmospheric pressure microplasma jet. Haiyun et al. [16] reported that effects of a helium flow in dielectric barrier discharge of atmospheric helium. Kanazawa et al. [17] studied that the microwave-induced microplasma jet was generated at atmospheric pressure using a modified waveguide-based plasma torch. The dynamics of the small size plasma jet was investigated by means of an ICCD camera. They observed the different plasma structures for argon and helium because the thermal conductivity of the discharging gas mainly affected the structure of the plasma jet. Ko et al. compared the gas flow rates and the gas temperatures obtained from numerical simulation and experiments [18] to clarify the basic characteristics of a pen-like atmospheric-pressure plasma. The relationship between gas flow rate and plasma behavior has not yet been clarified; this is a challenge in the application of atmospheric-pressure plasma. Studies on fluid control in plasma have been conducted. For example, Corke et al., used a dielectric barrier discharge (DBD) plasma jet actuator that proved to be effective in flow-separation control [19].

Apart from the investigations with respect to the electromagnetic properties, and the chemistry of the plasma, which are required in case of low-pressure plasma also, additional investigations with respect to the fluidity of the plasma have to be carried out in case of the atmospheric-pressure plasma. It is important to clarify the interaction of the atmospheric-pressure plasma with ambient gas species. Especially, this study focused on interaction between a filament plasma jet issuing from a microwave-excited plasma torch and a working gas flow which also passes around the plasma jet then issues from the plasma torch.

2. Experimental equipment and procedure

Fig. 1 shows the equipment used for processing atmospheric-pressure plasma in the experiment. The system consists of a 2.45-

* Corresponding author. Tel.: +81 26 269 5111; fax: +81 26 269 5130.
E-mail addresses: shouiio@shinshu-u.ac.jp (S. Iio), teshima@shinshu-u.ac.jp (K. Teshima), ezumi@ec.nagano-nct.ac.jp (N. Ezumi), ikeda21@shinshu-u.ac.jp (T. Ikeda).

0257-8972/$ – see front matter © 2011 Elsevier B.V. All rights reserved.
doi:10.1016/j.surfcoat.2011.09.013

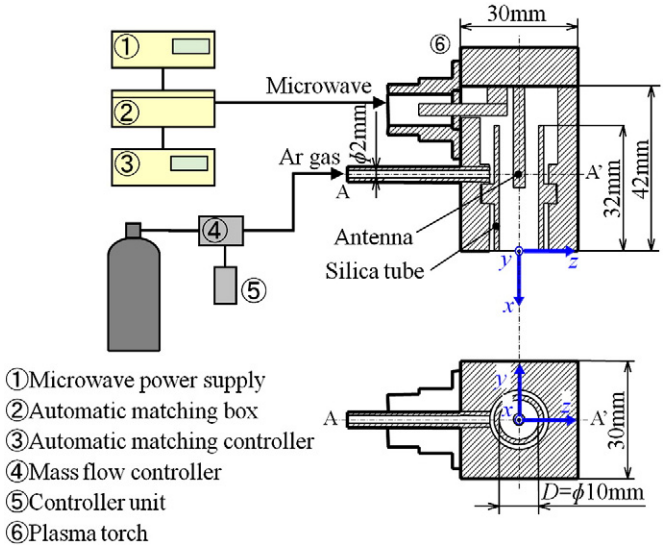

Fig. 1. Schematic illustration of experimental apparatus.

GHz microwave power supply (NJZ-2450, Nagano Japan Radio Co., Ltd.), a microwave matching box and its controller (NJZ-2451, NJRC), and a plasma torch (ser. no. 53P00192, NJRC). The plasma torch is connected to the automatic matching box using a coaxial cable, and the supplying microwave power to the generating device is set to 100 W. The discharged power of argon plasma jet was kept 20 W through the experiment. The plasma torch is made of aluminum and houses a silica tube and an antenna for detecting electric discharge. The silica tube is cylindrical with an inside diameter of 10 mm. The antenna is made of aluminum and has a diameter of 3 mm and a length of 26 mm. The working gas is argon. The supplying gas flow rate Q to the torch is controlled using a mass-flow controller. In this experiment, Reynolds number based on the torch exit diameter was changed from 4000 to 12,000 with changing the Q flux. The argon gas injected into the torch through the sidewall is then activated in order to produce plasma when the argon gas passes through the electric-discharge region near the end of the antenna; the plasma is then issued into the atmosphere. The origin of the coordinate system is set at the center of torch exit, the x is a position along the flow direction, the y-axis is perpendicular to the gas-supply tube, and the z-axis is along the direction of the gas-supply pipe. The torch exit is in the downward direction as shown in Fig. 1.

In this experiment, the images of the plasma jet were captured in the y-direction using a high-speed camera (FASTCAM-MAX, Photron). The shutter speed was set of 1/10,000 s. and the frame rate was 10,000 fps. The plasma jet behavior was evaluated by the image processing. The centerline of the plasma jet was extracted from many time-series images to measure the distance from the baseline, and then evaluated the dynamic fluctuation of the plasma jet. The gas flow field was visualized on the basis of the behavior of a tuft attached to the central portion of tip of the antenna. A silken thread with a length of 25 mm was used for the tuft. A constant-temperature anemometer and a single hot-wire probe were used for the gas velocity measurement. Platinum wire filament of 2.5 micrometer in diameter and 1 mm in length is used as hot-wire sensor. The probe is inserted into the flow downstream position by a handmade support without disturbing the flow. The sampling frequency was 10 kHz, and the sampling time was 10 s. However, it is difficult to measure the gas velocity when the plasma is present. Therefore, the gas velocity was measured in absence of the plasma, and the gas temperature, T, was measured in presence of the plasma, then the gas velocity was indirectly estimated from both results. A K-type thermocouple that was placed within a ceramic pipe with an external diameter of 1.3 mm was used for measuring the gas temperature.

3. Results and discussion

3.1. Visualization of plasma jet

Fig. 2 shows the visualized images of plasma jet. The plasma jet is injected downward from the bottom of the plasma torch. The images

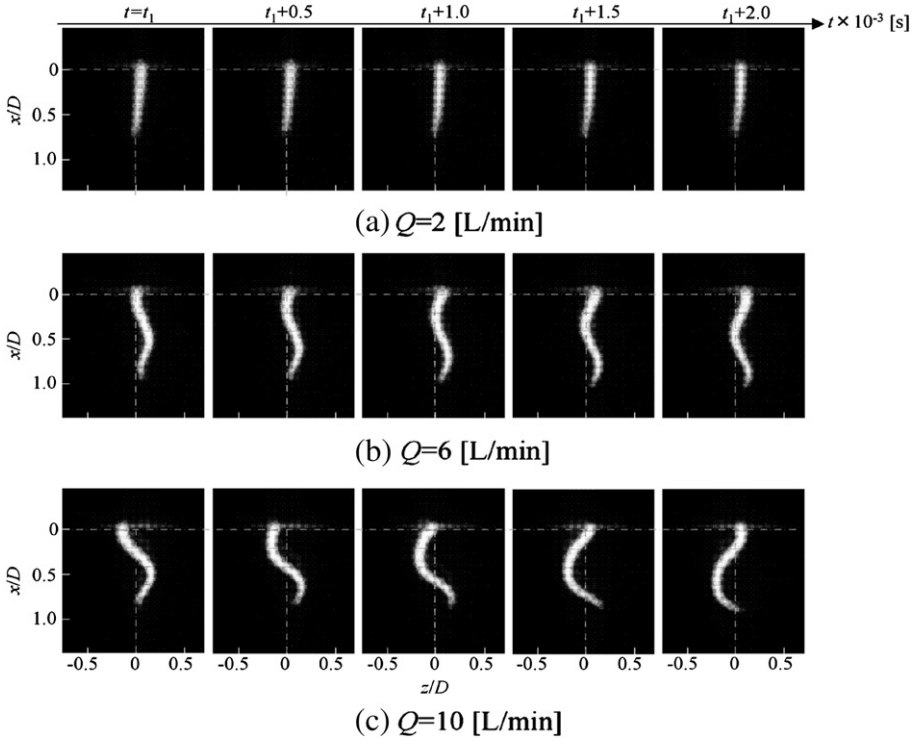

Fig. 2. Optical images of argon plasma jet.

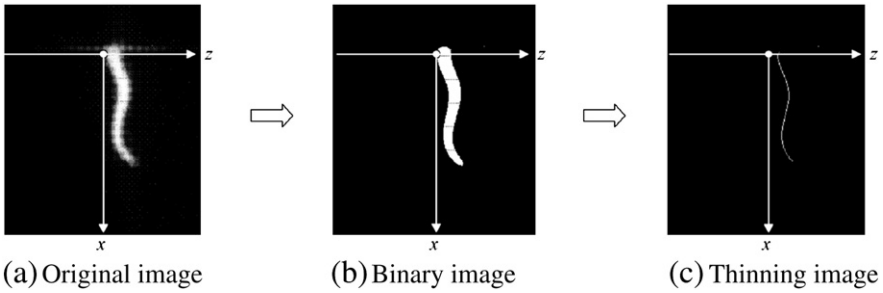

Fig. 3. Image processing.

in Fig. 2 are separated in time at intervals of 0.5 ms. At the most upstream part of the plasma jet, the plasma jet diameter is approximately 1.4 mm, which is equivalent to 14% of the inner diameter of the torch exit. This suggests that at any flow rate, the plasma extends from the top part of the antenna to approximately10 mm downstream from the torch exit. When $Q=2$ L/min (SLM) shown in Fig. 2(a), the plasma issues straight along the center axis of the torch, and its shape remains constant. In contrast, when $Q=6$ L/min and $Q=10$ L/min corresponding to Fig. 2(b) and (c), respectively, the plasma jet is meandering with time and moves along the x-axis. In addition, the figures show that the amplitude of the waving motion along the z direction increases with Q; it is due to the difference of Kelvin–Helmholtz instability in the jet shear layer. The plasma movement along the z direction, as shown in Fig. 2(c) is noteworthy. In the leftmost image, at $t=t_1$, issuing plasma position is shifted along the negative direction of the z-axis at the torch exit for $x/D=0$. Where, D is the inner diameter of the torch exit as shown in Fig. 1. The diameter is constant at 10 mm. After some time, the bias occurs along the positive direction of the z-axis. We observed a plasma sparkling position by the camera from the downstream of the torch, and then it was revealed that the position randomly moves on the circular surface at the tip of antenna. This is the origin of the meandering motion. The plasma was examined by creating an animation. The examination reveals that the deflection phenomenon also occurs along the y direction in an unsteady manner. Captured images were processed to evaluate quantitatively the deformation of the plasma jet. Fig. 3 shows the steps involved in image processing. First, the original plasma jet image shown in Fig. 3(a) is binarized as shown in Fig. 3(b). The threshold value in binarization was decided by the Otsu's method [20]. This is the optimal threshold selection method by the discriminant criterion, namely, so as to maximize the separability of the resultant classes in gray levels. Next, a thinning process is performed as shown in Fig. 3(c). Thinning is used to remove selected foreground pixels from binary image. By defining this line as the centerline of the plasma jet, its change of position along the z direction was plotted against time, as shown in Fig. 4. The thin and bold solid lines show the distances between the centerline of the plasma jet and the x-axis at $x/D=0.2$ and 0.4 ($x=2$ mm and 4 mm), respectively. This result shows that the fluctuation of the plasma jet along the z-direction is not periodic. The dominant frequency has not appeared even in the spectrum analysis. The dashed line in the graph shows the fluctuation of gas flow, which was monitored by the tuft method when the plasma was turned off. It is clear that the amplitude of gas flow is smaller than that of the plasma jet, and it is not observed the periodically fluctuation. This fact shows that the fluctuation of the plasma jet in the z-direction is not due to the flow field of argon gas. Here, note that there is a certain constant phase difference between Δz at $x/D=0.2$ and at $x/D=0.4$. In other words, the fluctuation of plasma jet at $x/D=0.2$ is reproduced at $x/D=0.4$ after a certain constant period of time. Therefore, it can be said that the wave motion of the plasma jet along the flow direction occurs at a constant speed.

Fig. 5 shows the root mean square value of the fluctuation of the plasma jet and the argon gas in the z-direction. $\Delta z_{T,rms}$ is an rms value of a fluctuation of the working gas in the z-direction which was obtained by tuft method. The amplitude $\Delta z_{T,rms}$ of argon gas, as measured by the tuft method, increases slowly with Q. In contrast, the amplitude Δz_{rms} of the plasma jet increases rapidly in the range $4\le Q\le 6$ L/min, and the rate of increase with increasing Q becomes constant at $Q\ge 6$ L/min. This result also suggests that the causal relationship between the fluctuation of the plasma jet and gas flow along the z-direction is small.

3.2. Gas flow velocity

The flow velocity distribution in the transverse direction indicates a top-hat profile in the near field of $x<20$ mm under our experimental conditions. This region is a potential core where the center velocity is constant. Thus the maximum velocity value is almost the same as averaged velocity except for a thin shear layer. In this region the admixture with the surrounding air is negligible because an entrainment rate is very small. Next, the gas flow velocity was measured in order to examine the interrelationship between the plasma jet and

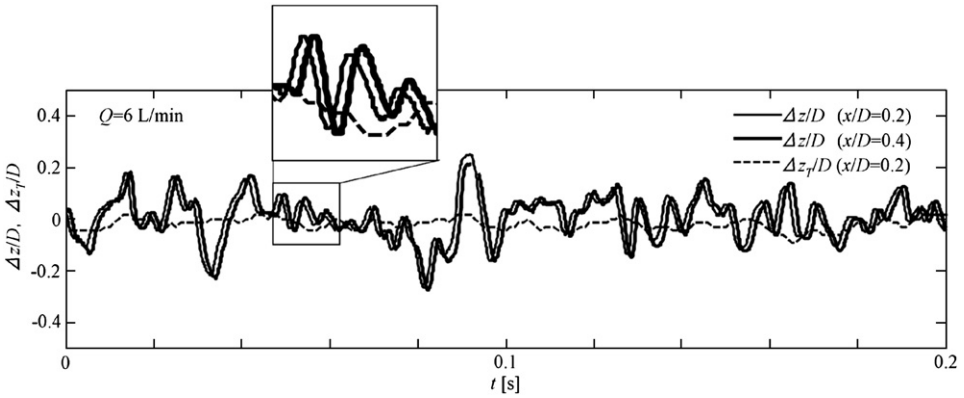

Fig. 4. Argon plasma jet and gas flow fluctuation.

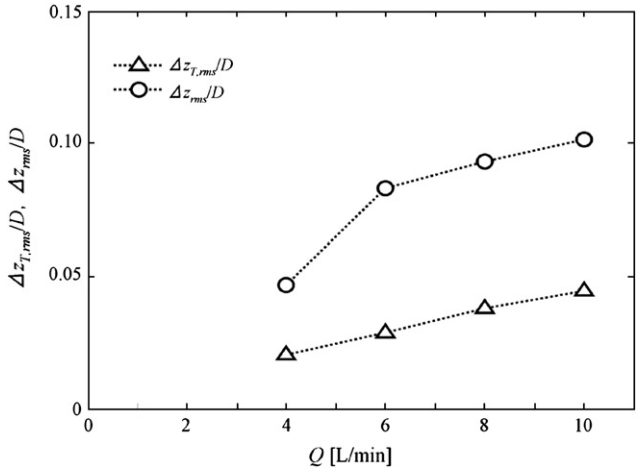

Fig. 5. RMS value of argon plasma jet and gas flow fluctuation with Q.

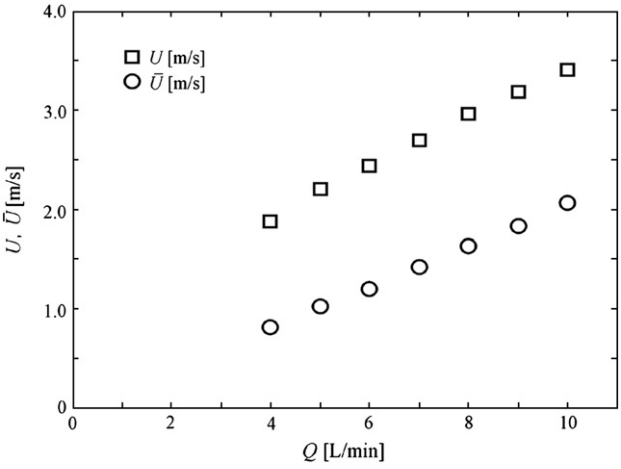

Fig. 7. Argon gas velocity with Q.

the gas flow. The measurement of the gas velocity is difficult due to the high temperature in the presence of the plasma. Therefore, we measured the gas velocity in the absence of the plasma jet at first, and then the velocity of heated working gas was estimated by calculation applying Charles's law which has taken consideration of the gas temperature, T, obtained by a thermo-couple measurement. Since, in the atmospheric-pressure plasma, the gas pressure at the torch exit is considered equal to the atmospheric pressure, the gas flow rate (velocity) is proportional to the gas absolute temperature. Fig. 6 shows a plot of the measured gas temperature against Q. The temperature was measured along the center axis (x-axis) at the just downstream of the torch exit where a thermocouple was placed at $x/D=2.0$ ($x=20$ mm), so that the thermocouple does not contact with the plasma jet. The measurement was repeated three times. The highest gas temperature recorded was $T=680$ K at $Q=3$ L/min. The gas temperature decreased as Q increased, and reached $T=470$ K at $Q=10$ L/min. In Fig. 7, the averaged gas velocity $\bar{U}$, which was measured three times when the plasma was turned off, and U, which was calculated velocity when the plasma was turned on, is plotted against Q. It is confirmed that while $\bar{U}$ increases in proportion to Q, the values of U was approximately 2.3 times at $Q=4$ L/min, and was 1.6 times greater than $\bar{U}$ at $Q=9$ L/min, respectively.

3.3. Advection velocity of plasma jet

We now focus on the relation between the advection velocity of the plasma jet and the gas velocity discussed in Section 3.2. The advection velocity of the plasma jet, $\bar{U}_P$, was obtained from the distance of two measurement points at $x/D=0.2$ and 0.4 divided by the phase rag as shown in Fig. 4. Further, the measurement was performed at $Q\geq 4$ L/min at which wave motions are observed. Fig. 8 shows the plasma advection velocity and the working gas velocity. Since the advection velocity may vary across measurements, 12 times measurement results are shown here with error bars. The result suggests that advection velocity of the plasma wave motion is roughly proportional to Q. It was revealed that the advection velocity is smaller than the working gas velocity in all flow rate conditions. In Fig. 9, the relation between the gas velocity, U, and the advection velocity of plasma, $\bar{U}_P$, is demonstrated with respect to Q. The data show that the advection velocity of the plasma jet is around 0.75 time the gas velocity at $Q=4$ L/min, and that the advection velocity approaches the gas velocity as the Q increases. Over the range considered in this experiment, the advection velocity of the plasma was 0.75–0.87 times the gas velocity. These results indicate that the behavior of the plasma jet is affected by the working gas motion, that is, the dynamic behavior of the plasma and the working gas will influence efficiency of surface treatment.

4. Conclusion

The visualization and the velocity measurement of argon atmospheric-pressure microplasma jet generated by the application of RF power of 2.45 GHz microwave were performed in this study. As a result, the unsteady sinusoidal waving motion in the radial direction of the torch was observed. The convection velocity of the plasma has a constant value in the just downstream region of the torch exit

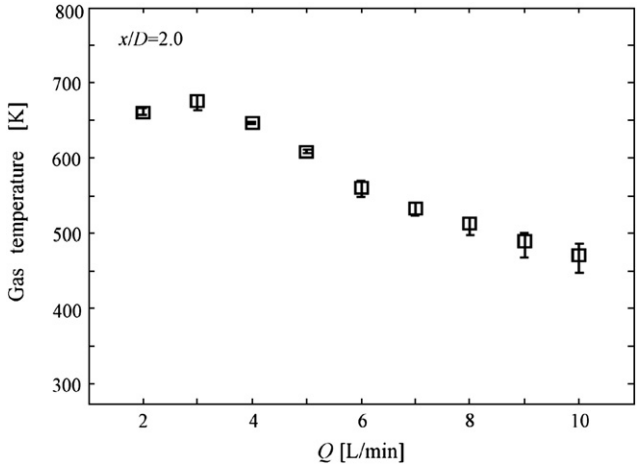

Fig. 6. Argon gas temperature with Q.

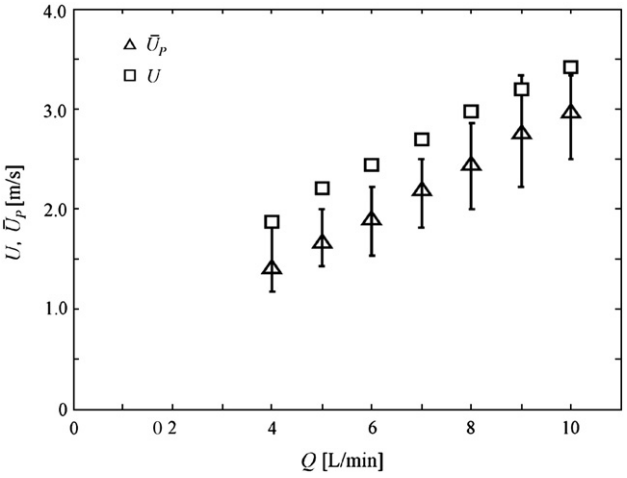

Fig. 8. Advection velocity of argon plasma jet and gas velocity with Q.

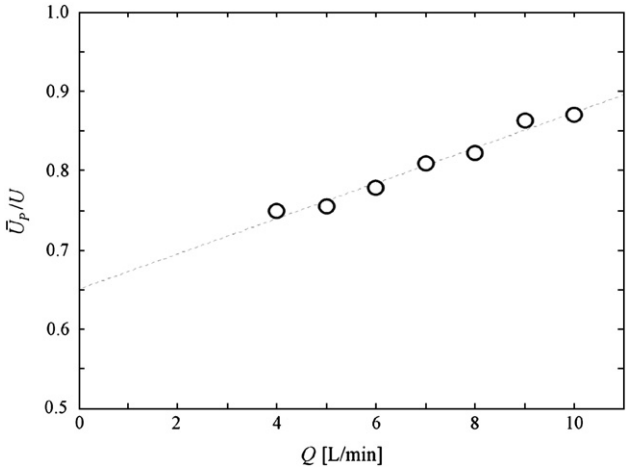

Fig. 9. Relation between gas velocity and advection velocity of plasma jet with *Q*.

while the supplying flow rate is kept constant, and the velocity ratio which is calculated as the plasma convection velocity divided by the averaged gas velocity. The velocity ratio is in the range of 0.75–0.87.

Acknowledgment

The assistance of Prof. Ohno, Nagoya University, is greatly appreciated. This work was partly supported by KAKENHI no. 22760126.

References

[1] A. von Engel, Ionized Gases, Clarendon Press, Oxford, 1955.
[2] Y. Raizer, Gas Discharge Physics, Springer Verlag, Heidelberg, 1991.
[3] M.A. Lieberman, A.J. Lichtenberg, Principles of Plasma Discharges and Materials Processing, John Wiley, New York, 1994.
[4] R. Hippler, H. Kersten, M. Schmidt, K.H. Schoenbach, Low Temperature Plasmas, Wiley-VCH, Weinheim, 2008.
[5] K.H. Becker, H. Kersten, J. Hopwood, J.L. Lopez, Eur. Phys. J. D60 (2010) 437.
[6] T. Sato, K. Fujioka, R. Ramasamy, T. Urayama, S. Fujii, IEEE Trans. Ind. Appl. 42 (2) (2006) 399.
[7] K.H. Becker, U. Kogelschatz, K.H. Schoenbach, R. Barker (Eds.), Non-Equilibrium Air Plasmas at Atmospheric Pressure, Applications of Atmospheric-Pressure Air Plasmas, IOP Publ., Bristol, UK, 2004.
[8] J. Schäfer, R. Foest, A. Quade, A. Ohl, K.D. Weltmann, Plasma Processes Polym. 6 (2009) S519.
[9] M.G. Kong, G. Kroesen, G. Morfill, T. Nosenko, T. Shimizu, J. van Dijk, J.L. Zimmermann, New J. Phys. 11 (2009) 115012.
[10] K.D. Weltmann, E. Kindel, T. Von Woedtke, M. Hähnel, M. Stieber, R. Brandenburg, Pure Appl. Chem. 82 (6) (2010) 1223.
[11] H.-H. Kim, A. Ogata, S. Futamura, IEEE Trans. Plasma Sci. 34 (3) (2006) 984.
[12] E. Havlíčková, O. Maršálek, R. Hrach, Eur. Phys. J. D 54 (2009) 313.
[13] S. Bornholdt, M. Wolter, H. Kerstena, Eur. Phys. J. D 60 (2010) 653.
[14] C. Oliveira, J.A. Souza Corrêa, M.P. Gomes, B.N. Sismanoglu, J. Amorima, Appl. Phys. Lett. 93 (2008) 041503.
[15] B.N. Sismanoglu, J. Amorim, J.A. Souza-Corrêa, C. Oliveira, M.P. Gomes, Spectrochim. Acta, Part B 64 (2009) 1287.
[16] Haiyun Luo, Zhuo Liang, Xinxin Wang, Zhicheng Guan, Liming Wang, J. Phys. D: Appl. Phys. 41 (2008) 205205.
[17] S. Kanazawa, R. Daidai, S. Akamine, T. Ohkubo, Surf. Coat. Technol. 202 (2008) 5275.
[18] T.-H. Ko, C.-M. Liu, Y. Matsuo, S. Ono, S. Teii, Int. J. Therm. Sci. 45 (2006) 681.
[19] T.C. Corke, E.J. Jumper, M.L. Post, D. Orlov, T.E. McLaughlin, AIAA Paper, 2002–0350, 2002.
[20] N. Otsu, IEEE Trans. Syst. Man Cybern. smc-9 (1) (1979) 62.